Journal of Physics and Chemistry of Solids 74 (2013) 354–359

Contents lists available at SciVerse ScienceDirect

Journal of Physics and Chemistry of Solids

journal homepage: www.elsevier.com/locate/jpcs

Spectroscopic characterization of mixed cation diphosphates of the type $M^{I}Fe^{III}P_2O_7$ (with M^{I}=Li, Na, K, Rb, Cs, Ag)

B.S. Parajón-Costa [a], R.C. Mercader [b], E.J. Baran [a,*]

[a] Centro de Química Inorgánica (CEQUINOR/CONICET, UNLP), Facultad de Ciencias Exactas, Universidad Nacional de La Plata, C. Correo 962, 1900 La Plata, Argentina
[b] Departamento de Física and Instituto IFLP (CONICET), Facultad de Ciencias Exactas, Universidad Nacional de La Plata, 1900 La Plata, Argentina

ARTICLE INFO

Article history:
Received 22 May 2012
Received in revised form
1 October 2012
Accepted 24 October 2012
Available online 3 November 2012

Keywords:
A. Inorganic compounds
B. Chemical synthesis
C. Infrared spectroscopy
C. Mössbauer spectroscopy
C. Raman spectroscopy

ABSTRACT

The mixed cation diphosphates of composition $M^{I}Fe^{III}P_2O_7$ have been prepared using the so called *co-precipitation method* starting with Fe(III) and M(I) nitrate solutions and solid $(NH_4)H_2PO_4$, and characterized by X-ray powder diffractometry. The infrared and Raman spectra of the compounds were recorded and the results are briefly discussed on the basis of their structural peculiarities. The ^{57}Fe-Mössbauer spectra show that the typical high-spin $Fe^{III}O_6$ octahedra existent in these compounds exhibit almost no distortion. However, the hyperfine parameters are sensitive to some characteristics of the M^{I} cations and to the different structural types.

1. Introduction

An important number of monovalent/trivalent cation diphosphates of stoichiometry $M^{I}M^{III}P_2O_7$ are known. In particular, for M^{III}=Fe^{III} materials with all the alkaline cations (Li–Cs), NH_4^+ and Ag^+ were characterized [1].

These phosphates pertain to three different structural types [1,2]. $NaFeP_2O_7$ presents two structures, a low temperature form, called $NaFeP_2O_7$-I [3,4], and a high temperature form, known as $NaFeP_2O_7$-II [3–6]. The potassium [3,7,8], rubidium [9,10], cesium [9,10] and ammonium [11] diphosphates belong to the $NaFeP_2O_7$-I form whereas $AgFeP_2O_7$ adopts the $NaFeP_2O_7$-II structure [12,13]. Finally, $LiFeP_2O_7$ posses a third, different structure [14,15].

During the years, these and other related diphosphates have awaked great interest in relation to its potential technological applications, as some of them may have unexpected magnetic [16,17] and useful catalytic [18,19] properties. Besides, recently some of them have been proposed as cathode materials for lithium batteries [20–22] and even, as nanoparticles, for decontamination and remediation of water [23].

Although the infrared spectra of these diphosphates have been reported and sometimes briefly discussed, the knowledge of their full vibrational-spectroscopic behavior remains incomplete as there is a lack of a detailed analysis of the IR spectra and the corresponding Raman spectra have never been investigated. On the other hand, vibrational spectroscopy is a powerful tool for the analysis and detection of structural peculiarities and differences.

Therefore, we have now prepared the $M^{I}FeP_2O_7$ diphosphates, with M^{I}=Li, Na, K, Rb, Cs and Ag, and recorded and discussed their IR and Raman spectra. In order to complement the spectroscopic characterization of these materials we have also measured and analyzed their ^{57}Fe-Mössbauer spectra in order to become an insight into the effects of the different Fe-environments on the hyperfine parameters.

2. Experimental

The synthesis of the six compounds was performed using the so called *co-precipitation method* [2,24], as follows: An equimolecular mixture of $Fe(NO_3)\cdot 9\cdot H_2O$ (10 mmol) and the corresponding $M^{I}NO_3$ (10 mmol) was dissolved together in 20 mL of distilled water, to which 10 drops of concentrated HNO_3 were added. To the gently heated solution, solid $(NH_4)_2HPO_4$ (20 mmol) was added in small portions, under continuous stirring. After completion of the addition, heating and stirring was maintained for half an hour more. The obtained precipitate was dried first over a water bath and then in an oven at 100 °C. The obtained powder was finally heated in a muffle furnace, rising the temperature very slowly up to 750 °C and maintaining at this temperature during 15–20 h, with some intermediate grindings.

* Corresponding author. Tel./fax: +54 221 4259485.
E-mail address: baran@quimica.unlp.edu.ar (E.J. Baran).

0022-3697/$ - see front matter © 2012 Elsevier Ltd. All rights reserved.
http://dx.doi.org/10.1016/j.jpcs.2012.10.012

The obtained diphosphates were characterized by X-ray powder diffractometry which showed, in all cases, the presence of the pure material, without detectable impurities.

The infrared spectra were recorded with a FTIR-Bruker-EQUINOX-55 spectrophotometer, using the KBr pellet technique. Raman spectra were obtained with the FRA 106 Raman accessory of a Bruker IFS 66 FTIR instrument, using the 1046 nm line of a solid state Nd:YAG laser for excitation. Spectral resolution for both measurements was $\pm 1\ cm^{-1}$.

Room temperature Mössbauer spectra were taken in transmission geometry using a conventional constant acceleration spectrometer of 512 channels with a 10 mCi nominal activity $^{57}CoRh$ source, in transmission geometry. The spectra were recorded in two ranges of velocities, namely, ± 12 mm/s and ± 4 mm/s. The absorber was a powdered sample, whose optimum thickness was calculated with the method of Long et al. [25]. The hyperfine parameters were obtained by fitting the data to lines of Lorentzian shape using a least-squares computer code with constraints. Isomer shifts were calibrated against an α-Fe foil at room temperature.

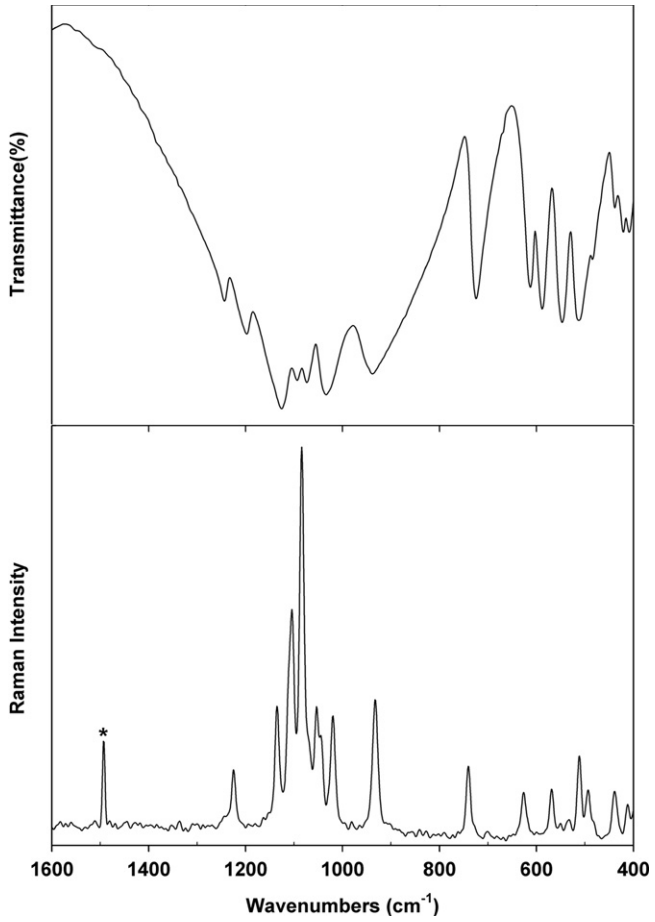

Fig. 1. FTIR (above) and FT-Raman (below) spectra of $AgFeP_2O_7$ in the spectral range between 1600 and 400 cm^{-1} (The medium intensity 1492 cm^{-1} Raman band originates in an instrumental noise).

3. Results and discussion

3.1. Crystal structure of the compounds

As mentioned above, the investigated diphosphates belong to three different structural types. $NaFeP_2O_7$ and $AgFeP_2O_7$ ($NaFeP_2O_7$-II structural type) crystallize in the monoclinic $P2_1/c$ with $Z=4$, whereas the $M^IFeP_2O_7$ (M^I=K, Rb, Cs) group ($NaFeP_2O_7$-I structural type) crystallize also in the same space group with $Z=4$. Despite this fact both groups are not isotypic, because there are small differences in the configuration of the P_2O_7 groups in the frameworks [2,9,26]. The host lattice of both structural groups, $[FeP_2O_7]$, is built from corner-sharing FeO_6 octahedra and P_2O_7 moieties. Each FeO_6 octahedron is linked to five different P_2O_7 groups, and each of these groups shares it six corners with five different FeO_6 octahedra and is bonded to one of them through bidentate bonding. This assemblage generate a 3D-framework with hexagonal tunnels filled by the M(I) ions, which are in ten-fold oxygen coordination. The two distorted PO_4 groups of each diphosphate unit are in staggered conformation, with an angular P–O–P bonding angle.

The remaining diphosphate, $LiFeP_2O_7$, crystallizes in the monoclinic space group $P2_1$ with $Z=4$. Also in this case each FeO_6 group is linked to five different P_2O_7 moieties, with one of them bonded in a bidentate fashion and the Li(I) ions are located in off-centered positions inside the tunnels presenting a pseudo-tetrahedral coordination. On the other hand, the diphosphate group exhibits an almost eclipsed conformation, with an angular P–O–P bonding angle [14].

3.2. Vibrational spectra of diphosphates belonging to the $NaFeP_2O_7$-I and $NaFeP_2O_7$-II structural types

As commented in the previous section, the $P_2O_7^{4-}$ anions present in these structural types present a staggered conformation with a non-linear bridge angle (C_s-symmetry). A total of 21 vibrational modes are expected for this conformation and all of them (13A′ and 8A″) are active in both, the infrared and Raman spectra [27,28]. On the other hand, since all ions are located at general C_1 positions in these crystal lattices, under site-symmetry

Table 1
Assignment of the IR and Raman spectra of $NaFeP_2O_7$ and $AgFeP_2O_7$ (band positions in cm^{-1}).

$NaFeP_2O_7$		$AgFeP_2O_7$		Assignments
Infrared	Raman	Infrared	Raman	
1256w, 1220w	1244w	1244w, 1198w	1225w	$\nu_{as}(PO_3)$ terminal stretch
1138vs, 1110w	1148m, 1117s	1126vs, 1094w	1136m, 1105s	
1083w	1092vs	1074w	1084vs	$\nu_s(PO_3)$ terminal stretch
1054sh, 1033vs	1074sh, 1028m	1034vs	1050m, 1038sh, 1020m	$\nu_{as}(PO_3)$ terminal stretch
935vs	931s	939vs	933s	ν_{as}(P–O–P) bridge stretch
736vs	753m	725vs	741m	ν_s(P–O–P) bridge stretch
625vs, 596vs, 555vs	637w, 582vw, 545vw	613s, 588s, 547s	625w, 569w, 535vw	$\delta_{as}(PO_3)$ terminal bend
519vs, 488vw	517w, 497w	513s, 484vw	511m, 490w	$\delta_s(PO_3)$ terminal bend
444sh, 427s, 418sh	447vw, 420vw, 405sh	438vw, 421w, 409w	443w, 415vw, 400vw	ρ(O′PO_3) rocking (cf.text)

vs, very strong; s, strong; m, medium; w, weak, vw, very weak; sh, shoulder.

conditions [28,29] all of them transform to A-species. Besides, as the unit cells contain four formula units, under factor group symmetry (C_{2h}) [28,29] a greater number of bands ($21A_g+21B_g+21A_u+21B_u$) is expected. From these, the phonons with *g*-parity are only Raman-active whereas those of *u*-parity are only IR-active. Notwithstanding, and as will be derived from the following discussion, the correlation-field effects have only a reduced impact on the infrared and Raman spectra.

As a typical example of the spectral patterns of the materials belonging to the $NaFeP_2O_7$-II structural type, Fig. 1 shows the FTIR and FT-Raman spectra of one of the investigated $AgFeP_2O_7$ samples, in the spectral range between 1600 and 400 cm^{-1}. The assignments for both $AgFeP_2O_7$ and $NaFeP_2O_7$ are given in Table 1, and briefly commented as follows:

- Comparing the IR and Raman spectra it was possible to identify, unambiguously, the symmetric stretching vibration of the terminal PO_3-moieties because this mode must be the most intense band in the Raman effect. Interestingly, this $\nu_s(PO_3)$ vibration appears intercalated between $\nu_{as}(PO_3)$ components. This situation has also been observed in other diphosphates [30,31] as well as in diarsenates [32] and divanadates [33].
- The total number of vibrations determined for the terminal PO_3-moieties fulfills exactly the theoretical expectations (a total of six vibrations: $4A'+2A''$) [27]. The weak 1038 cm^{-1} shoulder seen in the Raman spectrum of $AgFeP_2O_7$ and that of 1054 cm^{-1} in the FTIR spectrum of $NaFeP_2O_7$ probably originate in correlation-field effects.
- The two expected vibrations ($2A'$ modes) for the P–O–P stretching modes [27] are also observed in both spectra.
- In the bending region (including symmetric and antisymmetric deformation vibrations and PO_3-rocking modes against the bridge O-atom) a total of twelve bands is expected ($6A'+6A''$) [27]. From these, only eight bands could be identified in the measured spectral range, and we have followed the usual assignment $\delta_{as}(PO_3)>\delta_s(PO_3)$ [34–37]. On the other hand, the assignment in the region below 500 cm^{-1} is not straightforward because in this region not only O'PO_3 rocking modes, but also translational motions of the cations and other external modes are expected.
- Regarding the deformational mode of the bridge, for which only one A' species is expected in each spectra [27], it is usually assumed that it lies at relatively low energies, probably below or around to 200 cm^{-1} [27,28].

Fig. 2 shows the FTIR and Raman spectra of $RbFeP_2O_7$, in the spectral range between 1600 and 400 cm^{-1} as a typical example of the characteristic spectral patterns of the diphosphates belonging to the so-called low temperature form of $NaFeP_2O_7$ (or $NaFeP_2O_7$-I). The spectral assignment proposed for the three compounds belonging to this group is presented in Table 2 and is briefly commented as follows:

- In these cases the symmetric stretching vibration of the terminal PO_3 groups appear also intercalated between $\nu_{as}(PO_3)$ components, but the strongest Raman line, belonging to this vibrational mode, is that of highest energy. Therefore, it lies at higher energies in comparison to the values found in the previous analyzed structural group.
- The six predicted stretching modes of these terminal groups are not seen in all cases and especially in the Raman spectra which always display only four strong or very strong lines in this region.
- For the P–O–P stretching modes the two expected vibrations ($2A'$ modes) [27] are observed in both spectra, but in the case of $RbFeP_2O_7$ and $CsFeP_2O_7$ a weak splitting of the corresponding symmetric mode can be observed. In $CsFeP_2O_7$ also the antisymmetric bridge vibration shows a weak splitting
- In the lower energy region seven bands are found in both the IR and Raman spectra, in all cases.

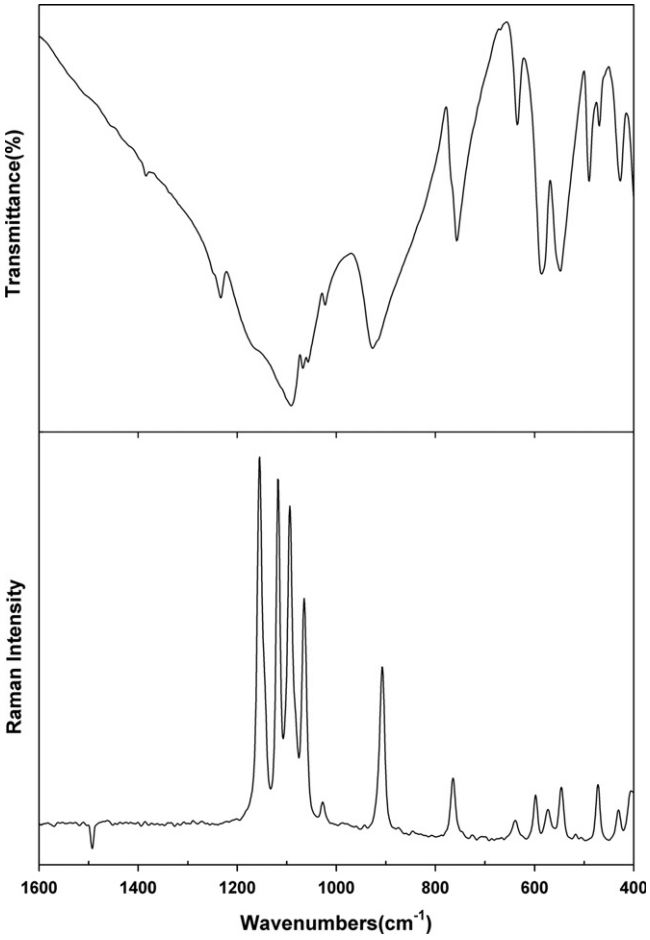

Fig. 2. FTIR (above) and FT-Raman (below) spectra of $RbFeP_2O_7$ in the spectral range between 1600 and 400 cm^{-1}.

3.3. *Vibrational spectra of $LiFeP_2O_7$*

As already mentioned, this compound has a nearly eclipsed conformation of the terminal PO_3 groups and an angular P–O–P bridge. Therefore, the symmetry of the "free" diphosphates group is, in this case, C_{2v} and the 21 vibrational modes are distributed as $4A_2+7A_1+4B_1+6B_2$ from which A_2 presents only Raman activity and all the others are active in both the IR and Raman spectra [27,28]. As under space group $P2_1$ all the ions are located at general C_1 positions in the crystal lattice and, under site-symmetry conditions [28,29] all the 21 vibrational modes transform to the IR and Raman active A-species. Under factor group symmetry (C_2) and $Z=4$ a greater number of bands may be expected ($42A+42B$) and all of them are IR and Raman active [28].

The FTIR and FT-Raman spectra of $LiFeP_2O_7$ in the spectral range between 1600 and 400 cm^{-1} are shown in Fig. 3 and the proposed assignment is presented in Table 3.

In this case, if the spectral analysis is performed on the basis of the site symmetry approximation, one can establish that the six expected components [27] for the terminal PO_3 groups are observed in the IR spectrum, whereas only four of them are

Table 2
Assignment of the vibrational spectra of $KFeP_2O_7$, $RbFeP_2O_7$ and $CsFeP_2O_7$ (band positions in cm^{-1}).

$KFeP_2O_7$		$RbFeP_2O_7$		$CsFeP_2O_7$		Assignments
Infrared	Raman	Infrared	Raman	Infrared	Raman	
1235w		1233w		1231w		$\nu_{as}(PO_3)$ terminal stretch
1144sh	1164vs	1170sh	1156vs	1162m,br	1141vs	$\nu_s(PO_3)$ terminal stretch
1097vs, 1065w, 1022w	1119s, 1098s, 1064s	1091vs, 1067w, 1057vw, 1022w	1119vs, 1094s, 1066s	1090vs, 1067w, 1057vw, 1024w	1120vs, 1091vs, 1065s	$\nu_{as}(PO_3)$ terminal stretch
933vs	910s	927vs	908s	929vs, 907sh	907vs	ν_{as}(P–O–P) bridge stretch
763vs	770m	766sh, 757vs	765m	764sh, 752vs	758m	ν_s(P–O–P) bridge stretch
639w, 585s, 553s	645w, 598m, 572w, 549m	634m, 586s, 548s	640w, 598m, 574w, 548m	628s, 590sh, 580vs, 554vs	632w, 598w, 569m, 543m	$\delta_{as}(PO_3)$ terminal bend
492m, 470w	472m	490m, 470w	473m	489s, 471w	475m	$\delta_s(PO_3)$ terminal bend
429m, 404w	438w, 406m	427m, 402m	431w, 406m	422s	425w, 401m	ρ(O'PO_3) rocking (cf.text)

vs, very strong; s, strong; m; medium; w, weak; vw, very weak; sh, shoulder; br, broad.

Table 3
Assignment of the vibrational spectra of $LiFeP_2O_7$ (band positions in cm^{-1}).

Infrared	Raman	Assignments
1227vw, 1170sh, 1125vs, 1098vw	1122s, 1105vs	$\nu_{as}(PO_3)$ terminal stretch
1075w	1073vs	$\nu_s(PO_3)$ terminal stretch
1032w	1037m	$\nu_{as}(PO_3)$ terminal stretch
970sh, 945vs	975w, 941m	ν_{as}(P–O–P) bridge stretch
761s	767sh, 761m	ν_s(P–O–P) bridge stretch
618m, 577s, 533s	618m, 559m, 537w	$\delta_{as}(PO_3)$ terminal bend
511s	512m	$\delta_s(PO_3)$ terminal bend
510s, 442s	520w, 448w, 427vw, 415vw	ρ(O'PO_3) rocking (cf.text)

vs, very strong; s, strong; m; medium; w, weak; vw, very weak; sh, shoulder.

observed in the Raman spectrum. Also in this case the $\nu_s(PO_3)$ mode appears again intercalated between $\nu_{as}(PO_3)$ components.

Concerning the two P–O–P bridge vibrations, they show weak splittings suggesting a certain activity of correlation-field effects.

For the terminal bending and rocking modes not all the twelve expected vibrations [27] are observed as only seven bands are found in the IR spectrum and eight in the corresponding Raman spectrum. Also, in this case it is difficult to perform a clear analysis in the lowest energy region.

In conclusion, the vibrational spectroscopic behavior of the three investigated structural groups is not too different, in agreement with the relatively small structural differences of the involved anionic $P_2O_7^{4-}$ moieties. In all cases, the symmetric stretching vibration of the terminal PO_3-groups appears intercalated between $\nu_{as}(PO_3)$ components. In addition, the mean value of these PO_3-stretching vibrations fulfills reasonably well a known empirical correlation between P–O bond lengths and stretching frequencies [38].

All the measured spectra show a scarce impact of correlation-field effects. Only a reduced number of bands showed weak splittings or shoulders which can be ascribed to such effects. In general, the spectra could be analyzed, without difficulties, on the basis of the "free" ion or site-symmetry approximations.

On the other hand, the presence of both bridge stretching vibrations in the measured IR and Raman spectra supports additionally the presence of angular P–O–P bridges in all the prepared materials [28,36,39]. In this context, both the IR and Raman data satisfy reasonably well the empirical correlation of Muck and Petru for P–O–P bridge frequencies [40]:

$$\nu_s(POP) = 0.32\nu_{as}(POP) + 430\ [cm^{-1}]$$

The results of this correlation, calculated from Raman data are presented in Table 4 and as it can be seen, in general, the calculated values are in relatively good agreement with those found experimentally with differences always below 7%. The best results are obtained for $LiFeP_2O_7$, $NaFeP_2O_7$ and $AgFeP_2O_7$ whereas a greater dispersion is found for the remaining three materials, belonging to the $NaFeP_2O_7$-I structural type.

Table 4
Values for ν_s(P–O–P) calculated from Raman data with the empirical formula of Muck and Petru [40] and compared with experimentally found values.

Diphosphate	$\nu_s(P–O–P)_{calculated}$	$\nu_s(P–O–P)_{experimental}$
$LiFeP_2O_7$	759	761
$NaFeP_2O_7$	728	736
$KFeP_2O_7$	721	770
$RbFeP_2O_7$	720	765
$CsFeP_2O_7$	720	758
$AgFeP_2O_7$	728	741

3.4. ^{57}Fe-Mössbauer spectra of the $M^IFeP_2O_7$ diphosphates

The room temperature Mössbauer spectra of the series $M^IFeP_2O_7$ (M^I=Li, Na, K, Rb, Cs, Ag) are shown in Fig. 4. The spectra obtained in the $\pm$12 mm/s velocities did not show any magnetic split signal. Hence, the central signals displayed by all the $\pm$4 mm/s spectra can be safely fitted to singlets or doublets of Lorentzian-shape lines. The values of the hyperfine parameters obtained after fitting are displayed in Table 5. All values of the isomer shift (δ) relative to α-Fe, belong to high-spin Fe(III) ions [41]. The δ- and Δ-parameters previously measured for the respective K-, Rb- and Cs-compounds [9] are in good agreement with the present values.

Although the isomer shifts for the compounds of different M^I cations are very similar (as a consequence of the structural framework of the FeO_6-octahedra with similar Fe–O distances linked through P_2O_7-units) a slight increase of δ when moving along the series from Li to Cs can be noticed. It reflects the decrease of the 3s electron density at the high-spin Fe(III) $3d^5$ ion

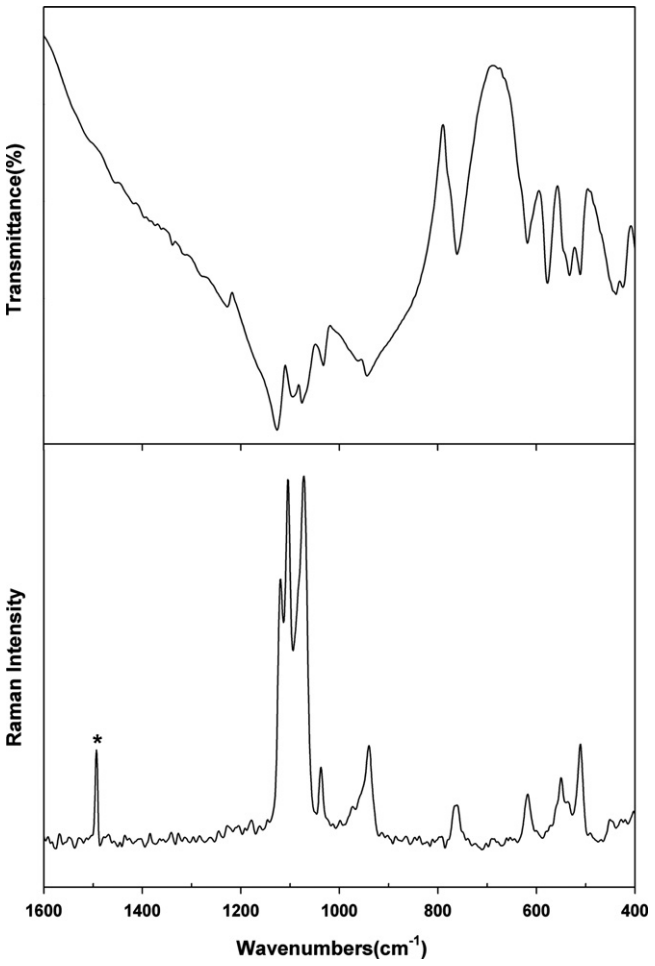

Fig. 3. FTIR (above) and FT-Raman (below) spectra of $LiFeP_2O_7$ in the spectral range between 1600 and 400 cm^{-1} (The medium intensity 1492 cm^{-1} Raman band originates in an instrumental noise).

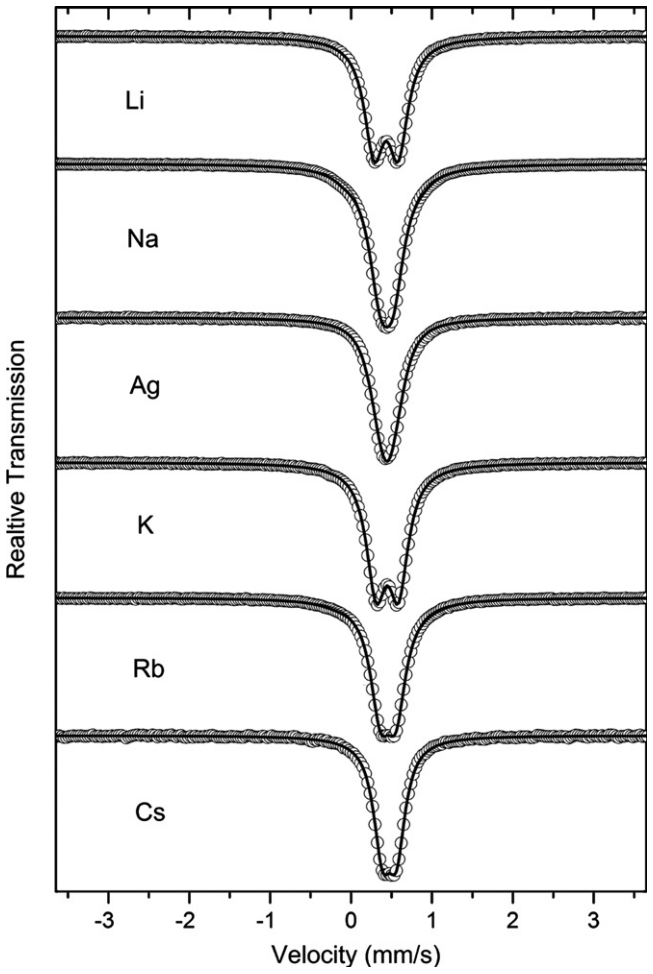

Fig. 4. Room temperature ^{57}Fe-Mössbauer spectra of the investigated diphosphates. The solid lines are the result of the fittings performed as described in the text.

nuclear sites. These differences might originate in the M^I–O^{2-} bond, which weakens when going from one cation to the next along the series Li→Na→K→Rb→Cs. Indeed, considering the Fe(III)–O–M(I) bonds, leaving aside the case of Ag(I), the cation interaction with the O^{2-} anion is known to weaken when moving along the series, which means that the oxide yields more easily charge density to the Fe(II) cation. This transfer would increase the Fe 3d electron density, which, on its own, would enhance the screening of the 3s electrons, thus lessening the effective density at the nuclear site.

The case of Ag(I) cannot be considered in line with the other cations because of the different Ag(I) behavior. In oxidic systems, the Ag(I)–O^{2-} bonds are always relatively strong due to the large polarizing power of Ag(I) (third Fajans' rule) [42] and its high Z_{efect} [43]. However, in the present study, its behavior is similar to that of Na(I) or K(I). This might be due to the fact that these M(I) cations are in a highly coordinated site (10) that might disturb the global polarizing power. It is also possible that, because the crystalline structure of $AgFeP_2O_7$ is of the $NaFeP_2O_7$-II type, the general trend for the series becomes slightly disrupted.

The measured values of the quadrupole splitting Δ show that the $Fe^{III}O_6$ octahedra present in these compounds are not greatly distorted. The values presented also in Table 5, follow a similar trend as the isomer shifts with the clear exception of the Na and Ag diphosphates. Although the valence contribution to the electric field gradient is small for Fe(III) ions, the differences observed for the different compounds of the series might arise from the same reasons that have already discussed for the isomer shifts for the case of the four compounds that follow the trend, i.e. Li→K→Rb→Cs. Considering only the valence term of the isomer shift, the weaker interaction of the M(I) cations with the oxide ions of the FeO_6 coordination polyhedra that agrees with the trend, would distort less the geometry of the polyhedron producing a smaller electric field gradient reflected in the smaller Δ-values. In addition, the size of the unit cells increases in the same direction, therefore contributing to a lower cation–oxygen interaction along the series.

The quadrupole splitting of the compounds $NaFeP_2O_7$ and $AgFeP_2O_7$, which do not fall in line with those of the other compounds, might be eventually related with the slightly

Table 5
Mössbauer parameters of the investigated compounds [δ is the isomer shift referred to an α-Fe foil at room temperature, Δ is the quadrupole splitting and Γ is the half-width at half-maximum Lorentzian line-width].

Diphosphate	δ (mm/s)	Δ (mm/s)	Γ (mm/s)
$LiFeP_2O_7$	0.43 ± 0.01	0.30 ± 0.01	0.28 ± 0.01
$NaFeP_2O_7$	0.44 ± 0.01	0.14 ± 0.01	0.29 ± 0.01
$AgFeP_2O_7$	0.45 ± 0.01	0.00 ± 0.01	0.38 ± 0.01
$KFeP_2O_7$	0.45 ± 0.01	0.28 ± 0.01	0.28 ± 0.01
$RbFeP_2O_7$	0.46 ± 0.01	0.20 ± 0.01	0.30 ± 0.01
$CsFeP_2O_7$	0.47 ± 0.01	0.18 ± 0.01	0.25 ± 0.01

different structure of these compounds in comparison to the K(I), Rb(I) and Cs(I) diphosphates. Also, the facts that $AgFeP_2O_7$ presents an almost nil quadrupole splitting and that the Δ-value of $NaFeP_2O_7$ is also smaller than in the other cases can probably be related also to a structural effect. One possible explanation is that in these cases a lattice term of opposite sign to that of the valence one might be induced at the Fe(III) sites, generating lower Δ-values.

4. Conclusions

These results are a contribution to a wider characterization of an interesting group of mixed cation diphosphates belonging to three different structural types. Very pure samples of the materials of composition $M^IFeP_2O_7$, with M^I=Li, Na, K, Rb, Cs, and Ag were obtained using a *chimie douce* procedure known as *co-precipitation* method. Their IR and Raman spectra were recorded and could be satisfactorily interpreted on the basis of the structural peculiarities of the $P_2O_7^{4-}$ moieties present in the crystal lattice. The ^{57}Fe-Mössbauer spectra show that the $Fe^{III}O_6$ octahedra present in these materials are not too distorted and the dependence of the hyperfine parameters on the different M^I-cations of the series can be related to the different features of the M(I)–O bonds and the structural peculiarities of the compounds.

Acknowledgments

This work has been supported by the Universidad Nacional de La Plata and the Consejo Nacional de Investigaciones Científicas y Técnicas de la República Argentina. B.S.P-C. and R.C.M. are members of the Research Career from this organization.

References

[1] A. Durif, Crystal Chemistry of Condensed Phosphates, Plenum Press, New York, 1995.
[2] J. Belkouch, L. Monceaux, E. Bordes, P. Courtine, Mater. Res. Bull. 30 (1995) 149.
[3] J.P. Gamondes, F. d'Yvoire, A. Boulle, C. R. Acad. Sci. Paris 272 (1971) 49.
[4] I. Grunze, H. Grunze, Z. Anorg. Allg. Chem. 512 (1984) 39.
[5] F. Gabelica-Robert, M. Goreaud, P. Labbé, B. Raveau, J. Solid State Chem. 45 (1982) 389.
[6] T. Moya-Pizarro, R. Salmon, S.L. Fournes, G. Le Flem, B.S. Wanklin, P. Hagenmüller, J. Solid State Chem. 53 (1984) 387.
[7] D. Riou, P. Labbé, M. Goreau, Eur. J. Solid State Inorg. Chem. 25 (1988) 215.
[8] G.S. Gopalakrishna, B.H. Doreswamy, M.J. Mahesh, M. Mahendra, M.A. Sridhar, J. Shashidhara Prasad, K.G. Ashmanajari, Bull. Mater. Sci. 28 (2005) 1.
[9] J.M.M. Millet, B.F. Mentzen, Eur. J. Solid State Inorg. Chem. 28 (1991) 493.
[10] E. Dvoncova, K.H. Lii, J. Solid State Chem. 105 (1993) 279.
[11] B.F. Alfonso, J.A. Blanco, M.T. Fernández-Díaz, C. Trobajo, S.A. Khainakov, J.R. García, Dalton Trans. 39 (2010) 1791.
[12] J. Belkouch, L. Monceaux, F. Oudet, E. Bordes, P. Courtine, Mater. Res. Bull. 25 (1990) 1099.
[13] K.V. Terebilenko, A.A. Kirichok, V.N. Baumer, M. Sereduk, N.S. Slobodyanik, P. Gütlich, J. Solid State Chem. 183 (2010) 1473.
[14] D. Riou, N. Nguyen, R. Benloucif, B. Raveau, Mater. Res. Bull. 25 (1990) 1363.
[15] G. Rousse, J. Rodríguez-Carvajal, C. Wurm, C. Masquelier, Solid State Sci. 4 (2002) 973.
[16] D. Maspoch, D. Ruiz-Molina, J. Veciana, Chem. Soc. Rev. 36 (2007) 770.
[17] M.-H. Whangbo, D. Daí, H.-J. Koo, Dalton Trans. (2004) 3019.
[18] J.M.M. Millet, J.C. Vedrine, Appl. Catal. 76 (1991) 209.
[19] P. Bonnet, J.M.M. Vedrine, C. Leclercq, J.C. Vedrine, J. Catal. 158 (1996) 128.
[20] Y. Uebou, S. Okada, M. Egashira, J.-I. Yamaki, Solid State Ionics 148 (2002) 323.
[21] H. Zhou, S. Upreti, N.A. Chernova, G. Hautier, G. Ceder, M.S. Whittingham, Chem. Mater. 23 (2011) 293.
[22] P. Barpanda, S.-I. Nishimura, A. Yamada, Adv. Energy Mater. 2 (2012) 841.
[23] E. Ordoñez Regil, N. García González, S.M. Barocio, Am. J. Anal. Chem. 3 (2012) 512.
[24] U. Schubert, N. Hüsing, Synthesis of Inorganic Materials, Wiley-VCH, Weinheim, 2000.
[25] G.J. Long, T.E. Cranshaw, G. Longworth, Mössbauer Eff. Ref. Data 6 (1983) 42.
[26] H.N. Ng, C. Calvo, Can. J. Chem. 51 (1973) 2613.
[27] A. Hezel, S.D. Ross, Spectrochim. Acta 23A (1967) 1583.
[28] S.D. Ross, Inorganic Infrared and Raman Spectra, McGraw Hill, London, 1972.
[29] A. Müller, E.J. Baran, R.O. Carter, Struct. Bonding 26 (1976) 81.
[30] G.T. Stranford, R.A. Condrate Sr, B.C. Cornilsen, J. Mol. Struct. 73 (1981) 231.
[31] E.J. Baran, R.C. Mercader, A. Massaferro, E. Kremer, Spectrochim. Acta 60A (2004) 1001.
[32] E.J. Baran, J.C. Pedregosa, P.J. Aymonino, J. Mol. Struct. 22 (1974) 377.
[33] E.J. Baran, I.L. Botto, J.C. Pedregosa, P.J. Aymonino, Monatsh. Chem. 109 (1978) 41.
[34] E. Steger, B. Kässner, Z. Anorg. Allg. Chem. 355 (1967) 131.
[35] E. Steger, B. Kässner, Spectrochim. Acta 24A (1968) 447.
[36] E.J. Baran, I.L. Botto, A.G. Nord, J. Mol. Struct. 143 (1986) 151.
[37] H. Bih, I. Saadoune, H. Ehrenberg, H. Fuess, J. Solid State Chem. 182 (2009) 821.
[38] L. Popović, D. De Waal, J.C.A. Boeyens, J. Raman Spectrosc. 36 (2005) 2.
[39] B. Jezowska-Trzebiatowska, Pure Appl. Chem. 27 (1971) 89.
[40] A. Muck, F. Petru, Z. Chem. 11 (1970) 29.
[41] F. Menil, J. Phys. Chem. Solids 46 (1985) 763.
[42] J.E. Huheey, E.A. Keiter, R.L. Keiter, Inorganic Chemistry. Principles of Structure and Reactivity, 4th Ed., Harper-Collins, New York, 1993.
[43] E.J. Baran, P.J. Aymonino, A. Müller, Z. Naturforsch. 24b (1969) 271.